Chapter 16
Nanoparticles: An Emerging Weapon for Mitigation/Removal of Various Environmental Pollutants for Environmental Safety

Gaurav Hitkari, Sandhya Singh, and Gajanan Pandey

Abstract Nanotechnology is a recent field of technology and nanoparticle materials are fundamental units that measure within the range 1–100 nm with several types of morphologies. They have exceptional and unique catalytic properties, which are associated with their size and are changed from their bulk materials. These nanoparticle materials are prepared by the various methods such as chemical, physical and biological methods. The prepared nanoparticles are investigated by numerous characterisation techniques such as X-ray diffraction (XRD), scanning electron microscopy (SEM), transmission electron microscopy (TEM), Brunauer–Emmett–Teller (BET) surface area analysis, absorbance spectroscopy, photoluminescence spectroscopy. XRD revealed the crystalline nature of the nanoparticles. SEM and TEM images provides information on the morphology and particle size distribution, and BET revealed the surface properties of the nanoparticles. Optical properties are investigated by absorbance and photoluminescence spectroscopic techniques. The effective photo-catalysis of organic toxic pollutants and heavy metals from the environment have been a challenging subject for human health. Much research has explored the environmental behaviour of nanostructured materials for the effective removal of hazardous organic pollutants and heavy metals, existing both in the surface and underground wastewater. The goal of this chapter is to indicate the outstanding removal capability and environmental remediation of nanostructured materials for various toxic organic pollutants and heavy metal ions.

Keywords Nanoparticles · Environmental contaminants · Nanoparticles synthesis · Waste management · Nanoremediation

G. Hitkari · S. Singh · G. Pandey (✉)
Department of Applied Chemistry, Babasaheb Bhimrao Ambedkar University (A Central University), Lucknow, Uttar Pradesh, India

R. N. Bharagava, P. Chowdhary (eds.), *Emerging and Eco-Friendly Approaches for Waste Management*, https://doi.org/10.1007/978-981-10-8669-4_16

1 Introduction

Nanotechnology is an emerging field of technology that covers a wide range of utilisation at nanoscale (1 nm = 10^{-9} m) dimensions, and a size range from 1 to 100 nm (billionths of a meter). Nanoparticles (NPs) are the most fundamental units of nanotechnology and comprise a group of tens of thousands of atoms measuring about 1–100 nm in vastly ordered crystalline way. Such NPs to the atom by atom; thus, the size and frequently the shape of a particle are composed of the preliminary conditions.

The requirement of nanotechnology to synthesise the desired shape and size of the nanomaterials for their convenient applications. Surfactants have been demonstrated to be the best shape-directing agents in the synthesis of nanomaterials, which is basically related to the surface adsorption of active molecules on different crystal planes of nucleating centers and thus, controlling their overall shape. Various types of surfactants have been adopted for the shape-limiting synthesis of nanomaterials, although ionic surfactants express clear shape-directing effects. Owing to the huge surface area to volume ratio, nanostructures display unique properties. The subbranches of nanotechnology in colloidal science, biology, physics, chemistry and other technical fields are associated with the explanation of phenomena and use of materials on the nanoscale (Mansoori 2002). This outcome was found in these materials and systems that often exhibit an arrative and extensively changing physical, chemical and biological properties by cause of their fine size, structure, and morphology. The distinctive properties of these nano-sized materials have resulted in the use of these nanomaterials in various fields (Fig. 16.1) like biomedicine, pharmaceuticals, cosmetics, surface-based sciences (Masciangioli and Zhang 2003).

In circumferential nanoscale science, engineering, technology, and nanotechnology contains investigation of imaging, calculating, modelling, and employing matter at this dimensional scale. Although in the industrial sectors nanostructures such as zinc oxide (ZnO) semiconductors are used in memory storage, display, optical,

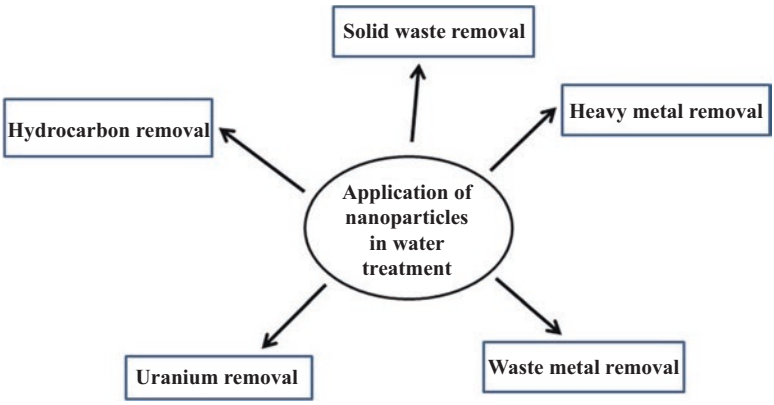

Fig. 16.1 Application of nanoparticles in water treatment in the environment

and photonic technologies; energy along with biotechnology; and in health care produces a considerable number of products containing nanomaterials, there are expanding achievements of nanotechnology to use in the environment as environmental technology to defend the environment from toxic waste, and remove the problems, which are present from the long-term use of hazardous waste materials.

Water is the most important substance for life on the earth and a valuable resource for human development. Finding reliable approaches to uncontaminated and cheap water is considered to be one of the truly fundamental humanitarian goals and remains a considerable worldwide challenge for the twenty-first century. Our present water supply faces many challenges, both old and new. Poisoning of water with lethal heavy metal ions such as Co(II), Cr(III), Cr(VI), (Hg(II), Pb(II), Ni(II), Cu(II), Cd(II), Ag(I), As(V) and As(III)) is attractive a brutal environmental and public health problem (Kumari et al. 2016; Yadav et al. 2017).

In nanotechnology, the profitable production of NPs has the potential to progress the environment, through the direct utilisation of those materials to distinguish, avoid and eliminate contamination, likewise indirectly by applying nanotechnology to intention cleaner manufacturing processes and generate environmentally accountable products. For example, ZnO, iron oxide (Fe_2O_3), cobalt oxide (Co_2O_3) and additional different NPs can eliminate contaminants from topsoil and ground water, and nanostructured sensors hold assurance for improved detection and tracking of contaminants.

These nanomaterials that deliver hygienic water from polluted water sources in both large scale and transportable applications and one that detects and cleans up eco-friendly contaminants (waste and toxic material), that is, remediation (Schrick et al. 2004; Liu et al. 2014). The word "remediate" means to resolve the problem and "bioremediation" means the procedure by which innumerable biological agents, such as bacteria, fungi, protists, or their enzymes are used to degrade the ecological impurities into less toxic forms (Van Dillewijn et al. 2007). The significant advantage of bioremediation over conventional treatments is that it is economical, highly proficient, reduces chemical and biological sludge, discriminates specific metals, there are no accompanying nutrient requirements, regeneration of biosorption and the probability of metal recovery (Kratochvil and Volesky 1998).

Research is required using nanoscale science and technology to identify opportunities and applications to environmental complications, and to estimate the potential ecological impacts of nanotechnology. Among the numerous applications of nanotechnology that have environmental implications, remediation of contaminated groundwater by using NPs containing zero-valent iron is one of the greatest conspicuous examples of a speedily developing technology with considerable potential benefits.

Oil spillage occurring during consideration, transportation, loading and filtering of rudimentary oil is a frequent phenomenon. Accidental oil tankers of crude oil on the surface of an enormous area of ocean currents for spreading and flora and fauna of the coastal shoreline and marine ecosystem have a huge impact. The oil factories and offshore piercing operations also release large amounts of crude oil/sludge, resulted in large-scale contamination of terrestrial and water resources. Unfinished

oil/petroleum gunk is a concoction of complexes such as aliphatic, aromatic, asphaltene and resin of hydrocarbons, which are well recognised for their injuriousness, and some of them are reported to be mutagenic and hazardous in nature. Contagion of the soil with lethal polyaromatic hydrocarbon (PAHs) results in extensive destruction of the biodiversity of flora and fauna, leading to reduction of the yield of products on land and contamination of ground water. In view of these problems, valuable remediation of petroleum hydrocarbons to develop a cost-effective and environmentally friendly technology is a very important need.

The dimension of the nanomaterials is involved in particles with at least one dimension measuring between 1.0 and 100 nm. Some definite characteristics such as high surface-to-volume ratio, enhanced magnetic and special catalytic properties etc. (Gupta et al. 2011) make these nanomaterials/ NPs far more advantageous than their majority phase counterparts in the field of remediation technology. The high surface area and surface reactivity of nanomaterials compared with their corresponding bulk material facilitate their remediation of the contamination at a fast rate with reduced amounts of dangerous by-products (Bhattacharya et al. 2013). A miscellaneous arrangement of nanomaterials such as carbon nanotubes (CNTs), nanoscale zeolites, dendrimer enzymes, biometallic particles and metal oxides are now being used for decontamination of polluted sites (Mehndiratta et al. 2013). The application of multi-walled carbon nanotubes has been working to eliminate organic contaminates such as PAHs and polychlorinated biphenyls (PCBs) (Shao et al. 2010). Zhang (2003) reported a comprehensive list of pollutants that can be potentially remediated by using iron (Fe) NPs. By the application of these NPs in enzyme-mediated remediation, technology is steadily gaining ground because NPs provide a biocompatible and inert microenvironment, that interferes least with the inherent properties of the enzymes and helps in recollecting their biological accomplishments (Ansari and Husain 2012). In addition, the magnetic properties of the NPs enable an easy separation of immobilised enzymes or proteins from the reaction mixtures by simply applying a magnetic field. Thus, there is no need for centrifugation or purification which, otherwise, continues the procedural inconsequence and operational complications (Khoshnevisan et al. 2011). In the remediation procedure, there are some selective nanomaterials used for the remediation process, which is a crucial step, as they may be toxic for the microorganisms (Rizwan et al. 2014).

2 Synthesis of Nanomaterials

2.1 Chemical Method for the Synthesis of Nanoparticles

Various chemical methods are applied for the fabrication of nanostructure materials such as controlled precipitation, sol–gel synthesis, hydrothermal reactions, sonochemical reactions, reverse micelles and micro-emulsion technology, hydrolysis

and thermolysis of precursors. For the wastewater treatment such as removal of toxic metal applications, a suitable surface alteration of the nanostructures is a critical characteristic concerning both discrimination and aqueous solidity of these materials. To this end, ZnO has been an interesting metal oxide for study by several researchers. Organic and inorganic functionalised Fe_3O_4 NPs have been established and modifications of the synthesis methods mentioned above have been proposed.

2.1.1 Mechanochemical Process

The mechanochemical process is an inexpensive and humble process of finding large amounts of NPs. In this method, high-energy dry milling is used, because it initiates a reaction through ball-powder influences in a ball mill, at a low temperature, and a "thinner" is added to the system in the form of a solid (such as NaCl), which acts as a medium for the reaction and separates the NPs being formed. The most important problem in this process or method is a uniform crushing of the powder and reduction of the particles to the required size, which decreases with increasing time and energy of grinding. Inappropriately, a longer grinding time leads to a greater quantity of impurities. The benefits of this method are the low costs of fabrication, small particle sizes and the restricted tendency of particles to agglomerate, in addition to the high uniformity of the crystalline structure and morphology.

2.1.2 Controlled Precipitation

The controlled precipitation is a commonly used method for the production of ZnO nanostructures as it makes it possible to obtain a product with repeatable properties. This method involves the fast and spontaneous reduction of a zinc precursor solution by introducing a reducing agent, to limit the progression of particles with specified dimensions, followed by the precipitation of a precursor of ZnO from the solution. The next step in this method, the precursor of this salt undergoes thermal treatment, followed by grinding to eliminate impurities. It is very challenging to break down the agglomerates that form; thus, the powder is calcinated at a high temperature to have a high level of agglomeration of particles. In the precipitation process, the precipitation is controlled by parameters such as pH, temperature and time of precipitation.

The aqueous solution of zinc acetate and zinc chloride is applied for the preparation of ZnO (Kołodziejczak-Radzimska et al. 2010). In this technique, the controlled parameters subsumed the concentration of the reagents, the flow of the addition of substrates, and the reaction temperature. A ZnO NP was formed with a uniform particle size distribution and a huge surface area.

Another method of effective precipitation of ZnO was implemented by Wang et al. (2010). Nanometric ZnO NPs were obtained by precipitation from aqueous

solutions of NH_4HCO_3 and $ZnSO_4 \bullet 7H_2O$ by way of the following reactions (16.1) and (16.2):

$$4ZnSO_{4(aq)} + 10NH_4HCO_{3(aq)} \rightarrow Zn_5\left(CO_3\right)_2\left(OH\right)_{6(s)} 5\left(NH_4\right)_2 SO_{4(aq)} + 8CO_{2(g)} + 2H_2O \quad (16.1)$$

$$Zn_5\left(CO_3\right)_2\left(OH\right)_{6(s)} \rightarrow 5ZnO_{(s)} + 2CO_{2(g)} + 3H_2O_{(g)} \quad (16.2)$$

This study was implemented using a membrane device containing two plates of polytetrafluoroethylene, with stainless steel as a spreading medium. The size of ZnO NPs was 9–20 nm with a narrow range of particle size obtained by this method. On the basis of X-ray diffraction (XRD) investigation, both the precursor and the ZnO itself were revealed to have a wurtzite structure. The size and shape of material was influenced by varying the temperature, calcination time, flow rate and concentration of the supply phase.

The iron oxide or magnetite NPs are synthesised by a stoichiometric combination of the iron precursor of ferrous and ferric salt of iron in an aqueous medium. The residue of Fe_3O_4 is collected at a pH value between 8 and 14. The desired shape and size of the NPs can be made precise by modifying the nature of the salts, ionic strength, temperature and pH (Schwarzer and Peukert 2004; Jolivet et al. 2004). The NPs achieved by this method are rang in size from 5 to 100 nm. The size of the NPs is controlled by the addition of carboxylate ions (e.g. citric, gluconic, or oleic acid) or polymer surface complexing agents (e.g. dextran, carboxy dextran, starch, or polyvinyl alcohol) and surfactant also used for the size control of particles during the formation of magnetite (Laurent et al. 2008).

2.1.3 Sol–Gel Method

The preparation of ZnO nanopowder using the chemical sol–gel method is an interesting subject with regard to the ease, low cost, consistency, repeatability and relatively mild conditions of synthesis, which facilitate the surface variation of ZnO with particular organic compounds. These variations in properties extend its range of applications. The ZnO nanopowder obtained by this method give very advantageous optical properties of NPs and has become a simple and modern topic of research, as reflected in several scientific publications (Mahato et al. 2009). There are two methods of synthesis using the sol–gel method: first, the formation of films from a sol, and second, powder from a sol is transformed into a gel.

The sol–gel method was also used to obtain nanocrystalline ZnO by Ristić et al. (2005). The solution of tetramethylammonium hydroxide (TMAH) was added in to a solution of zinc 2-ethylhexanoate (ZEH) in propan-2-ol. The resulting suspension solution stood for 30 min (otherwise for 24 h) and then washed with water and fine ethanol. TMAH is a powerful organic base, which compared with an inorganic base (e.g. sodium hydroxide [NaOH]) is characterised by a pH of ~14. At such a high pH value, metal oxides are not affected with the cation present in the base, which may

have an influence on the ohmic conductance of the oxide material. The consequence of the extent of ZEH used and the growing time of the colloidal solution were determined.

2.1.4 Hydrothermal Reactions

The hydrothermal synthetic technique does not concern the use of organic solvents or additional handling of the product such as crushing and calcination, which makes it a very simple and ecologically friendly technique. The synthesis of the NP by this method takes place in an autoclave, where the combination of substrates is heated gradually to a temperature of 100–300 °C and left for numerous days. As an outcome of heating followed by refrigeration, crystal nuclei are formed, which then propagate. So many advantages of this process, together with the possibility of carrying out the synthesis at very low temperatures, the different shapes and measurements of the resulting crystals depend upon the composition of the starting reaction mixture and the reaction temperature and pressure, the high degree of crystallinity of the product, and the high level of cleanliness of the material gained (Djurisic et al. 2012; Innes et al. 2002).

Chen et al. (1999) reported the synthesis of ZnO NPs by the hydrothermal method by using the reagents $ZnCl_2$ and NaOH in a ratio of 1:2, in an aqueous solution. The process takes place by way of the reaction (16.3):

$$ZnCl_2 + 2NaOH \rightarrow Zn\left(OH\right)_2 \downarrow + 2Na^+ + 2Cl^- \tag{16.3}$$

The white precipitate of $Zn(OH)_2$ was obtained by purification and washing, and then the pH was adjusted to a value of 5–8 using HCl. In the autoclave hydrothermal method, heating takes place at a programmed temperature for a set time, followed by cooling. The end product of the reaction process is ZnO with the following reaction (16.4):

$$Zn\left(OH\right)_2 \rightarrow ZnO + H_2O \tag{16.4}$$

Fe_3O_4 NPs synthesised by the hydrothermal method have been reported in the literature over the last decade (Daou et al. 2006; Wang et al. 2004; Mizutani et al. 2008). Synthesis of these materials using this method is performed in aqueous media in reactors or autoclaves where the pressure can be higher than 2,000 psi and the temperature can be greater than 200 °C. The synthesis of magnetite NPs uses the hydrothermal method in two main ways: hydrolysis and fine oxidation or neutralisation of mixed metal hydroxides. These two reactions are very analogous, except that only ferrous salts are used in the first method. This process, on the basis of reaction conditions, such as solvent, temperature and time, frequently has significant effects on the products or compounds. The particle size of the material is controlled primarily through the rate procedures of nucleation and grain growth in the hydrothermal method.

2.1.5 Solvothermal Method

Zhang et al. (2010) reported the ZnO NPs synthesised using the solvothermal method in the symmetry of globules and non-solid globules with the existence of an ionic liquid such as imidazolium tetrafluoroborate. The authors recommended that the solvothermal process may involve subsequent chemical reactions such as (16.5) and (16.6):

$$2\left(1-\mathrm{x}\right)\mathrm{OH}^{-}+2\mathrm{xF}^{-}+\mathrm{Zn}^{2+}\rightarrow \mathrm{Zn}\left(\mathrm{OH}\right)_{2-2\mathrm{X}}+\mathrm{F}_{2\mathrm{x}} \tag{16.5}$$

$$\mathrm{Zn}\left(\mathrm{OH}\right)_{2-2\mathrm{X}}\mathrm{F}_{2\mathrm{x}}\rightarrow \mathrm{ZnO}_{1-\mathrm{x}-\mathrm{y}}\mathrm{F}_{2\mathrm{x}}\left(\mathrm{OH}\right)_{2\mathrm{y}}+\left(1-\mathrm{x}-\mathrm{y}\right)\mathrm{H}_{2}\mathrm{O} \tag{16.6}$$

The hollow sphere shape of ZnO NPs is obtained with the diameters of 2–5 μm and channels approximately 10 nm in diameter existing and similarly achieved in the sample or material. The breadth of the wall of such a sphere was approximately 1 μm. The arrangement proposed by Zhang et al. may conglomerate the properties of both a solvothermal hybrid and an isothermal system. It can be estimated that a solvothermal hybrid and an isothermal system may be successfully handed down to prepare novel materials with remarkable properties and morphologies.

2.1.6 Reverse Micelles and Micro-emulsion Technology

The classic definition of an emulsion as a continuous liquid phase in which a second, discontinuous, immiscible liquefied stage is dispersed is far from complete. On the basis of the nature of the external phase, one very appropriate method for categorising emulsions is first to divide them into two broad groups. The two groups are generally called oil-in-water (O/W) and water-in-oil (W/O) emulsions. According to this definition, almost any highly polar, hydrophilic liquid falls in to the "water" category, whereas hydrophobic, non-polar liquids are considered an "oil" (Kołodziejczak-Radzimska et al. 2012; Li et al. 2009).

Vorobyova et al. (2004) used emulsion structures in their research work. ZnO NPs were precipitated in an inter-phase reaction of zinc oleate (liquefied in decane solvent) with NaOH used as a precipitating agent (liquefied in ethanol [C_2H_5OH] or water as a solvent). In the complete process, the following reaction is involved (16.7):

$$\mathrm{Zn}\left(\mathrm{C}_{17}\mathrm{H}_{33}\mathrm{COO}\right)_{2}\left(\mathrm{decane}\right)+2\mathrm{NaOH}\left(\mathrm{water\,and\,ethanol}\right)\rightarrow \mathrm{ZnO}+\mathrm{H}_{2}\mathrm{O}+2\mathrm{C}_{17}\mathrm{H}_{33}\mathrm{COONa} \tag{16.7}$$

On the basis of scanning electron microscopy (SEM) and XRD, analysis was performed on the ZnO nanopowder obtained by this method, subsequent elimination of the solvents and exposure to air at room temperature. It was found that the reaction may possibly take place in different phases, mutually in water and in the organic

phase. The magnitude of the NPs and the situation of their phase are affected by the reaction circumstances such as temperature, substrate and ratio of two-phase components. Vorobyova et al. reported ZnO NPs achieved by this method with dissimilar particle shapes (irregular aggregates of particles, needle shapes, nearly spherical and nearly hexagonal forms, and spherical aggregates) and with the magnitude of: 2–10 μm, 90–600 nm, 100–230 nm and 150 nm respectively, contingent on the reaction process conditions.

There are also numerous additional methods available designed for the synthesis of NPs (ZnO), including development from a gas phase, a pyrolysis spray method, a sonochemical method, synthesis by using microwaves, in addition to several other methods.

2.1.7 Chemical Vapour Deposition

The chemical vapour deposition (CVD) method is mostly used in the semiconductor industry for setting down narrow films of numerous materials. It is essentially a chemical procedure. In this process, the precursors decompose on the substrate or reactant and produce the preferred deposit. In the CVD process, at a prominent temperature, the evaporated precursors are adsorbed onto a substance surface through vaporised precursors hosted in a CVD reactor. In the CVD process, evaporated originators are prepared to adsorb onto a substance surface detained at a high temperature. Crystals are produced by this method through adsorbed molecules, react with other or decompose. Several steps are involved in this process:

- Starting materials are transported on the growth surface by a boundary layer.
- Chemical reactions take place on the growth surface.
- By-products formed by the gas-phase reaction have to be removed from the surface. A homogeneous and assorted nucleation process takes place in the gas phase.

2.2 Physical Method for the Synthesis of Nanoparticles

2.2.1 Physical Vapour Deposition Method

Physical vapour deposition approaches are used for the deposition of narrow films of metals onto different surfaces. This technique includes condensation from the cloud phase. Three main steps are included in this process.

- By the sublimation of the disappearance of a material corresponding to the vapour phase.
- Shipping of the material to the starting material from the source.

- Progress of the narrow film and constituent parts by nucleation and progression. The source disappears because of the consuming electron beams, thermal energy, the sputtering technique and cathode arc plasma.

2.2.2 Mechanical Ball Milling Method

The mechanical ball milling method is used as a solid-state preparation and is frequently performed by the using ball milling equipment that is commonly divided into a "low energy" and a "high energy" category based on the value of the induced mechanical energy to the powder mixture (Boldyrev and Tkáčová 2000). The main purpose of the grinding process in this method is to decrease the size of the particles and unification of the particles in new phases. The different kind of ball milling process can be used for the fabrication of nanomaterials in which the balls leave an impression upon the powder charge (Yadav et al. 2012).

High-energy ball milling is an appropriate technique for fabricating nano-sized powders. Inter-metallic NPs synthesised by this method constitute the most common method reported in the literature. Previously, a motorised milling process was started; the powder of nanomaterial was loaded together with numerous heavy balls (steel or tungsten carbide) into a container. By energetic shaking or high-speed gyration, a high level of mechanical energy was applied to the powder because of collision with heavy balls (Ghorbani 2014).

2.2.3 Laser Ablation Method

Pulsed laser ablation deposition (PLD) is an eye-catching synthetic method owing to its capability to produce NPs with fine size dissemination and near to the ground level of contaminations. In laser ablation, a synthetic method with three main steps is involved and materialisation of nanomaterials from a target absorbed in liquid. In the laser pulse method, the first step is to heat up the target surface to boiling point, and thus, a plasma column containing vapour atoms of the target is generated. Then, the plasma enlarges adiabatically, and as a final point, NPs are produced when the condensation process occurs. So many synthetic parameters such as laser wavelength, laser energy, pulse width, liquid media type and ablation time affect the characteristics of the products formed by this method.

In 2010, aluminium NPs were fabricated using the pulsed laser ablation method of Al targets in ethanol, acetone and ethylene glycol. The comparison between ethanol and acetone decided through the reaction elucidated that acetone medium produced finer NPs (the magnitude of NPs is 30 nm) with thinner size distribution (from 10 to 100 nm) (Baladi and Mamoory 2010). Hur et al. reported the synthesis of Mg-Al and Zn-Al-layered double hydroxide by using laser ablation in the liquid technique. Ordinary thicknesses of these structures were about 500 nm and the breadth of a single layer was approximately 6.0 nm (Hur et al. 2009).

2.2.4 Gas Evaporation Method

This method is most frequently used for the synthesis of NPs by the evaporation of originator materials from the molten state into a chamber occupied by an inert gas, where the vaporous metal condenses. The nanomaterials obtained by this process and its properties are strongly affected by the purity and type of the originator or precursor used as a starting material, and the transparency of the inert gas atmosphere. A modified inert gas evaporation method is known as cryomelting and can also be used for the formation of NPs. In the cryomelting procedure, the disappearing metal is hurriedly condensed in the region and cooled to about 70 K. A magnitude of NPs of 20–200 nm is produced using this method.

In 2010, the materialisation of aluminium NPs by a unique electromagnetic levitational gas condensation (ELGC) system was planned and manufactured. The greatest frequency of flow of argon for the fabrication of aluminium NPs was found to be 10–15 l/min (Kermanpur et al. 2010).

2.3 Biological Method for the Fabrication of Nanoparticles

The recent and the most innovative area of research is synthesis of nanomaterial by the enormous diversity of marine resources. Over a decade, for the fabrication of low-cost, energy-efficient and non-hazardous NPs, so many variations of microorganisms and plants are used. The biological method used for the fabrication of NPs is known as "green synthesis" or "green chemistry" techniques. Selected plant sources such as *Avena sativa*, *Azadirachta indica*, Aloe vera, *Tamarindus indica* leaf extract and *Cinnamomum camphora* are used for the fabrication of NPs. The different microorganisms used on behalf of the fabrication of NPs such as bacteria, fungi, actinomycetes bacteria, yeast and virus have already been reported by many researchers. Few specimens of NPs fabricated by different micro-organisms including *Aspergillus fumigates* (Ag NPs), *Candida glabrata* (CdS NPs), *Fusarium oxysporum* (silver, gold, zirconia, cadmium sulphide, silica and titanium particles, in addition to CdSe quantum dots), *Pseudomonas aeruginosa* (Au NPs), and many others (Nirmala et al. 2013). The broad area of application of biologically synthesised NPs is shown in Fig. 16.2.

2.3.1 Biosynthesis of Gold Nanoparticles

The biological method is used for the fabrication of gold NPs by using an oceanic sponge *Acanthella elongata* at an extracellular level. In this procedure, the sponge extract was added to 10^{-3} M $HAuCl_4$ aqueous solution at 45 °C; then, the colour of this solution changed to pinkish ruby red colour solution. By the continuous stirring of this solution, 95% of the bioreduction of $AuCl_4$- ions occurred within 4 h and generated unvarying gold NPs. The morphology and magnitude of these gold NPs

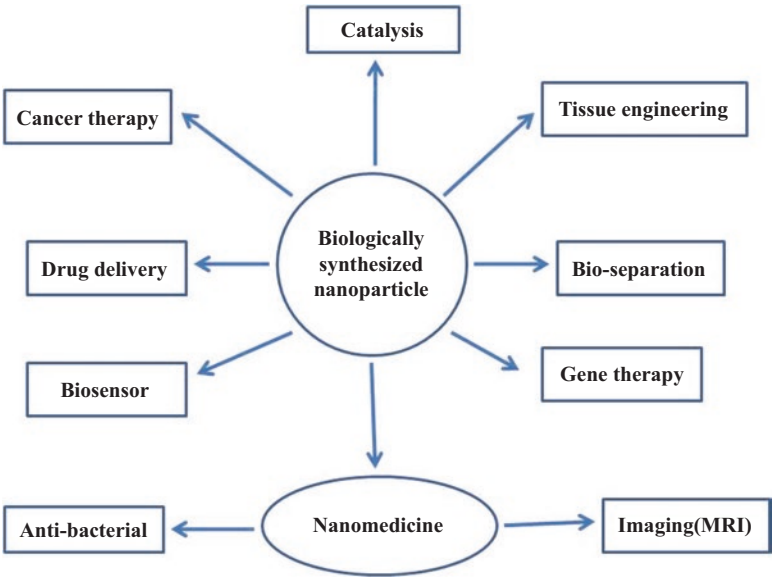

Fig. 16.2 Application of bio-synthesised nanoparticles

obtained by this method is monodisperse, globular, ranging in size from 7 to 20 nm and about 25% are 15 nm in diameter. This was confirmed by high-resolution transmission electron microscope (HR-TEM). From XRD investigation the NPs achieved by this method are crystalline in nature. The extract of aquatic sponge *Acanthella elongata*, possibly acting as the capping agent, is used for the prevention of agglomeration of the NPs and for their stabilisation. It was furthermore identified that the water-soluble organics existing in the extract were included in the reduction of gold ions. Josephine et al. reported that the synthesis of extremely steady gold NPs was achieved by biotransformation using various species of marine sponges (Josephine et al. 2008) (Table 16.1).

3 Nucleation and Growth of Nanoparticles

For many years, the nucleation and growth procedure of NPs have been defined through the LaMer burst nucleation (LaMer and Dinegar 1950) and the variation in the particles size was described by Ostwald ripening (Ostwald 1900). The modern model of this accepted process was developed by the Lifshitz–Slyozov–Wagner (LSW) theory (Lifshitz and Slyozov 1961; Wagner 1961) and was first exhibited by Reiss (1951). This theory was thought to be the only one on nucleation until that of Watzky and Finke (1997), moving toward constant slow nucleation followed by autocatalytic growth. On the basis of empirical formulas, ultraviolet (UV)-visible spectroscopy is a common technique for the determination of the particle size of

Table 16.1 Synthesis of nanoparticles by biological methods

Marine source	Nano-particle synthesised	Size and shape
Sargassum wightii (alga)	Gold	8–12 nm, mostly thin planar structures, some are spherical
Yarrowia lipolytica NCIM 3589 (yeast)	Gold	Particle size varied with varying concentration. Mostly spherical nanoparticles, some hexagonal or triangular nanoplates
Fucus vesiculosus (alga)	Gold	Both size and shape varied according to different initial pH values
Acanthella elongata (sponge)	Gold	7–20 nm, spherical
Penicillium fellutanum (fungi)	Silver	5–25 nm, spherical
Brevibacterium casei MSA19 (sponge associated)	Silver	Uniform and stable
Pichia capsulata (yeast)	Silver	5–25 nm, spherical
Rhodopseudomonas palustris (photo-synthetic bacterium)	Cadmium sulphide	8.01 ± 0.25 nm, cubic crystalline structure

quantum dots. In modern study, by the use of small angle X-ray scattering and a liquid cell within a TEM, it has been possible to further probe NPs in situ and acquire comprehensive information on how NPs grow in solution (Thanh et al. 2014). There are various theories of nucleation and growth, but some of the principles of what happens within the various processes are described.

3.1 LaMer Mechanism

The theoretical separation of the nucleation and growth process into binary stages by using the LaMer mechanism which is the first mechanism. The sulphur sols obtained from the decomposition of sodium thiosulphate was studied by the LaMer, which involved two steps: in the first step, unrestricted sulphur was formed from thiosulphate; in the second step, the sulphur sol is formed in the solution. The procedure of nucleation and development over and done with the LaMer mechanism can be separated into three portions.

1. In the first step the concentration of permitted monomers rapidly increases in the solution.
2. In the second step, these highly concentrated monomers undergoes "burst-nucleation" which is responsible for the reduction in the concentration of free monomer in the solution. The rate of this process is explained as "effectively infinite" and after this point, there is no nucleation occurring because of the low concentration of monomers.
3. In the last step, nucleation growth occurs under the control of the diffusion of the monomers through the solution.

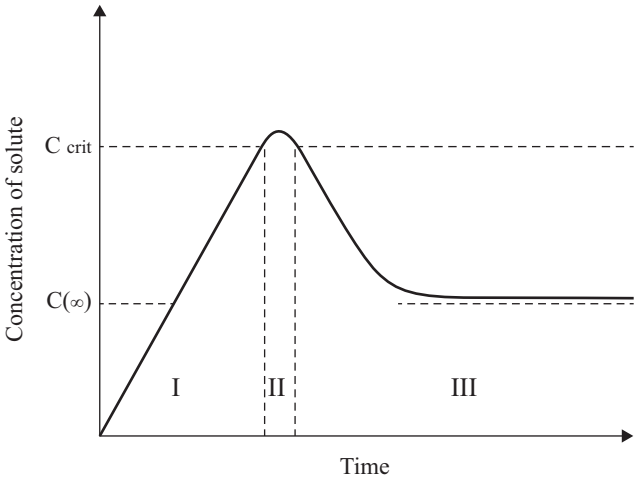

Fig. 16.3 Schematic representation of the LaMer diagram

The three phases are shown in Fig. 16.3 (Sugimoto 2007) where the concentration of the monomers is schematically plotted as a function of time.

3.2 Ostwald Ripening and Digestive Ripening

The Ostwald ripening mechanism (Wagner 1961) was first described in 1900. The growth mechanism is affected by the variation in solubility of NPs dependent on the magnitude of the particles, which is described by the Gibbs–Thomson relation, Eq. (16.8).

$$C_r = C_b \exp \frac{2\gamma v}{\mathrm{rk}_b T} \tag{16.8}$$

In this equation, Cr is the solubility of the particle, C_b is the concentration of bulk solution, γ is surface energy, v is the molar volume of the bulk crystal, r is the spherical radius of the particle, k_b is Boltzmann's constant and T is temperature. Owing to the extraordinary solubility and the high surface energy of slighter particles inside the solution, these re-dissolve and allow the larger particles to propagate even more. The calculated theory of Ostwald ripening inside a close system is described by Lifshitz and Slyozov (Reiss 1951) and Wagner (Watzky and Finke 1997).

Digestive ripening is effectively the contradiction of Ostwald ripening. In the former, minor particles propagate at the expense of the larger ones and has been described by Lee et al. (2005), where an applicable form of the Gibbs–Thomson equation, Eq. (16.8), is derived. This manner of formation is controlled once for a second time by the surface energy of the particle inside the solution where the larger particle re-dissolves and in turn less significant particles grow.

4 Characterisation

The characterisation technique of materials is important for understanding their properties and applications. This chapter defines the instruments and experimental set-ups utilised for various measurements toward the characterisation of the synthesised nanomaterials. The techniques adopted to characterise the NPs are: SEM, TEM, XRD, Fourier transform infrared spectroscopy (FTIR), UV-visible spectroscopy, photoluminescence spectroscopy and the Brunauer–Emmett–Teller (BET) technique. TEM and SEM give information about the particle size, shape, topology and their distribution. For the identification of crystal structure and particle size determination, the XRD technique is used. Identification of a functional group existing in the material was characterised by FTIR spectroscopy. Electron microscopy is a powerful and modern technique that allows investigation of the morphology and properties of a solid surface body with a high resolution, that employs beams of fast-tracked electrons and different versions of probe microscopes. Optical properties of material are studied using UV-visible and fluorescence spectra. The BET technique is used for the analysis of the surface area and pore size distribution of material by the N_2 adsorption–desorption isotherm and Barrett–Joyner–Halenda plot.

4.1 X-Ray Diffraction

The physical properties of material, thin film, chemical composition and crystallographic structure is defined by the very convenient characterisation tool of the XRD technique. The XRD characterisation technique has the potential to provide information on an anatomical scale, specifically for crystalline species. The several structural material goods of the crystalline phase such as imperfection structure, strain, particle magnitude and phase composition are measured using this technique. This characterisation determines the thickness of film, but also arrangement in amorphous material. The crystallite size of the nanomaterials is also calculated using this technique. XRD graph is shown in Fig. 16.6.

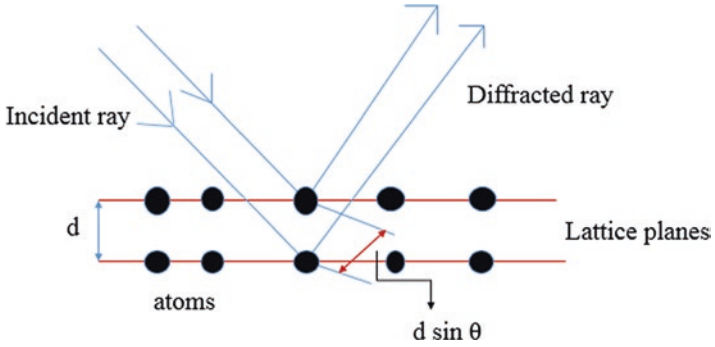

Fig. 16.4 Schematic representation of a Bragg's Low

4.1.1 Basic Principle

The basic principle of XRD is founded on the constructive interference of monochromatic X-rays from a crystalline sample. A cathode ray tube produces X-rays filtered to generated monochromatic radiation, collimated and focused in the direction of the sample. The X-rays first and foremost interact with electrons present in atoms, strike, and some photons from the incident beam are deflected away from the original. The diffraction pattern of the sample is produced by constructively and destructively interfering X-rays formed on the detector. The incident X-ray radiation produces a Bragg peak if their mirror image from the numerous planes interfere constructively. The interference is constructive when the phase shift is a multiple of 2λ; this situation can be expressed by Bragg's law:

$$n\lambda = 2d\sin\theta$$

where n is an integer, λ is the wavelength of the incident wave, d is the spacing between the planes in the atomic lattice and sin θ is the angle between the incident ray and the scattering planes. A schematic illustration of XRD is presented in Fig. 16.4.

4.1.2 Instrumentation

The instrumentation of a typical powder X-ray diffractometer includes of a source of radiation, a monochromator to select the wavelength, slits to modify the outline of the beam, a sample and a detector. The position of the detector and the reasonable adjustment of sampling occurs by use of a goniometer. The goniometer mechanism supports the sample and detector, permitting accurate movement. The source of X-rays contains a number of components; the most common being Kα and K_β. The particular wavelengths are the main characteristics of the target material (Cu, Fe, Mo, Cr). Monochromators and filters are used to absorb unwanted emission with

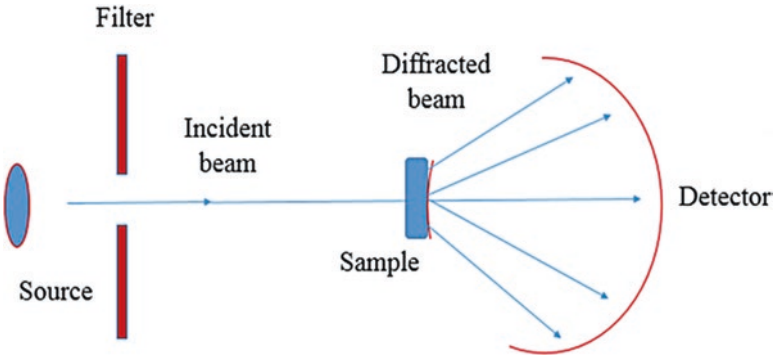

Fig. 16.5 Schematic representations of X-ray diffraction (XRD)

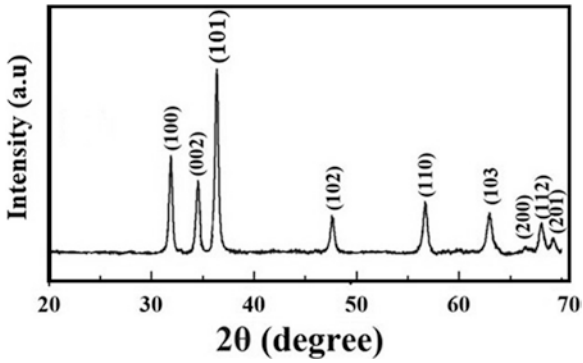

Fig. 16.6 Schematic representation of XRD graph of ZnO

wavelength Kα, while allowing the desired wavelength, K_{β}, to pass through. The X-ray radiation most frequently used in this procedure is that radiated by copper, whose specific wavelength for K_{β} radiation is equal to 1.5418 Å. The filtered X-rays are collimated and concentrated onto the sample, as presented in Fig. 16.5. When the incident beam attacks a powder sample, diffraction take place in a probable orientation of 2θ. The diffracted beam is detected by using a moveable detector such as a Geiger counter, which is attached to a chart recorder. The counter is fixed for examination over a range of 2θ values at a constant angular velocity. Routinely, a 2θ range of 5°–70° is sufficient to cover the most beneficial part of the powder pattern. The scanning speed of the counter is usually 2θ of 2° min^{-1}. A detector records and progresses this X-ray signal and changes the signal to a count rate, which is then fed into a device such as a printer or computer monitor. The sample must be ground to a fine powder, before loading it into the glass sample holder. The sample should completely occupy the square glass well. In the current work, XRD patterns were noted using Rigaku X-ray diffractometer (RINT-2200) with CuKα radiation at a 0.02°/s step interval.

XRD graphs are shown in Fig. 16.6.

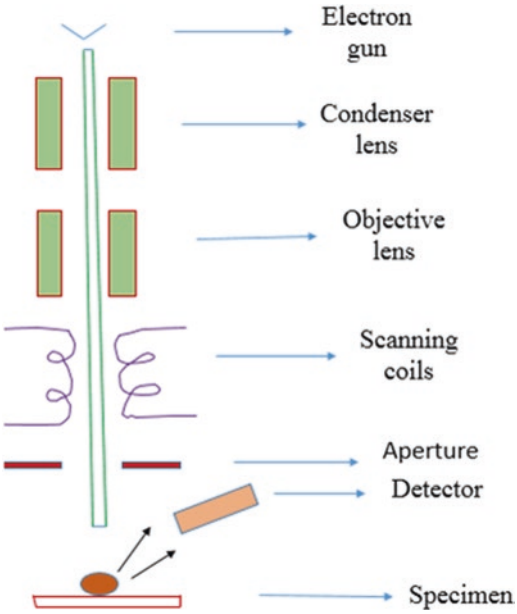

Fig. 16.7 Schematic representation of scanning electron microscopy (SEM)

4.2 Scanning Electron Microscope

4.2.1 Basic Principle

Scanning electron microscopy (SEM) is a very valuable imaging technique that applies a ray of electrons to obtain high-intensification images of specimens. The SEM maps the reflected electrons and allows imaging of thick (~mm) samples. SEM images are manufactured by rastering (scanning) a beam over the sample and developing the image point by point.

4.2.2 Instrumentation

The highly magnified image is produced by using electrons instead of light to form an image with the SEM instrument. A schematic illustration of SEM is revealed in Fig. 16.7. The electron gun produces a beam of electrons at the top of microscope. The electron beam monitors a perpendicular path through the microscope, which is held within a vacuum. The stream of electrons travels through electromagnetic fields and lenses, which centre the beam down in the direction of the sample. Once the electron beam forays the sample, electrons and X – rays are turned out from the sample. These X-rays, backscattered electrons and secondary electrons are collected through the detectors and transform them into a signal that is shown on a

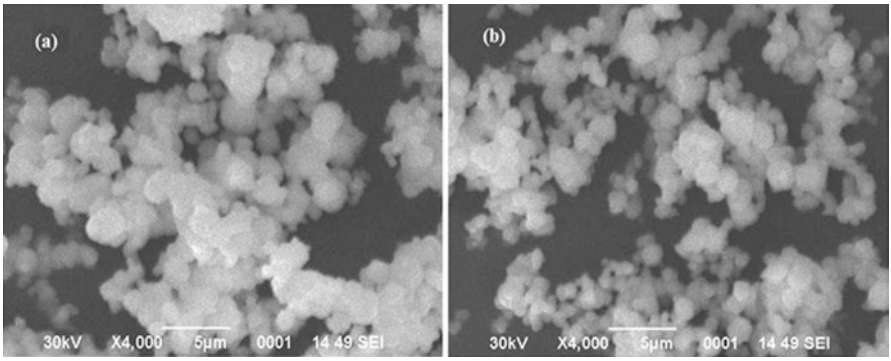

Fig. 16.8 Schematic representation of a SEM image

screen such as a television screen. This produces the finished image. In this research work, the powder samples were placed on the carbon tape, which was attached to the sample holder. JEOL JSM 6320F (FESEM), F E I Quanta FEG 200 (HRSEM) were used to study the surface morphology of the sample.

Investigation with SEM is considered to be "non-destructive"; that is, X-rays generated by electron interactions do not lead to volume damage of the sample; thus, it is probable that the same materials are evaluated repeatedly (Egerton 2005). The SEM images the surface structure of bulk samples, from the biological, medical, materials sciences, and earth sciences up to magnifications of ~×100,000. The images have a greater depth of field and resolution than optical micrographs, making them ideal for rough specimens such as fracture surfaces and particulate materials. Some SEM images are shown in Fig. 16.8.

4.3 Transmission Electron Microscopy

4.3.1 Basic Principle

Transmission electron microscopy (TEM is a very useful technique for nanomaterials. It technique provides information about the diameter and a highly magnified transmitted image of the material. In this technique, the electron beam is transmitted with an ultra-thin specimen, then acting together with the specimen as it permits via this interaction the formation of an exceedingly magnified image. The detection of the image by passes electrons through the sample. The shorter wavelength of electrons compared with photons can therefore provide a greater resolution than conventional light microscopes. TEM can provide two distinct types of information about a specimen: a magnified image and a diffraction pattern.

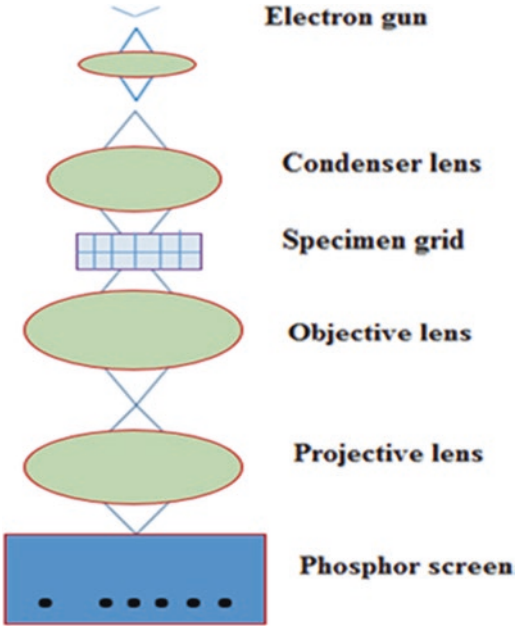

Fig. 16.9 Schematic representation of transmission electron microscopy

4.3.2 Instrumentation

The instrumentation of TEM includes four parts: electron source, electromagnetic lens system, sample holder and imaging system, as shown in Fig. 16.9. The electron beams generated through the source are forcefully focused by the electromagnetic lenses and the metal apertures. In this system, the electrons allow a slight energy range to pass through, so that the electrons in the electron beam have a definite energy. This electron beam drops on the sample located in the holder. In this system, the electron beam is permitted through the specimen. This transmitted ray reproduces the patterns on the sample. This transmitted beam is projected onto a phosphor screen. In the current work, TEM images were recorded by a JEOL JEM 2100F transmission electron microscope at an accelerating voltage of 200 kV. The images were obtained using this technique, the powdered samples were dispersed in ethanol solvent and it was ultrasonicated for 20 min. The copper grid in this instrument is coated in the dispersed compound and TEM images were found.

4.4 Brunauer–Emmett–Teller Technique

The Brunauer–Emmett–Teller (BET) technique is the most common method for defining the surface area of powders and porous materials. This technique is also used for calculating pore volume, pore radius and pore size dissemination of

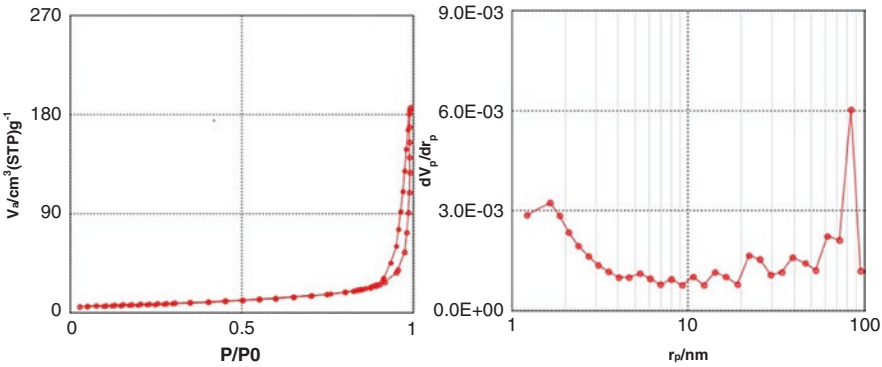

Fig. 16.10 (**a**) N_2 adsorption desorption plot (**b**) Barrett–Joyner–Halenda plot

nanomaterials. Nitrogen is the most commonly employed gaseous adsorbate used for surface probing by BET methods. For this reason, standard BET analysis is most often conducted at the boiling temperature of N_2 (77 K). The surface area of the material is calculated from the measured monolayer capability and knowledge of the cross-sectional area of the molecule being used as a probe. For the instance of nitrogen, the cross-sectional area is taken as 16.2 Å2/ molecule. The adsorption-desorption and BJH plot are shown in Fig 16.10.

4.4.1 Instrumentation

Brunauer–Emmett–Teller experiments are characteristically conducted to a relative pressure, P/P_0, of approximately 0.3 at 77 K, where P_0 is the saturation pressure (Lowell et al. 2004). The relative pressure in terms of relative humidity can be considered, i.e. the experiment is conducted to 30% of the saturation pressure of N_2 at 77 K (≈230 torr). At comparative pressures above the point at which an N2 monolayer has formed on the solid, capillary condensation is found within the pore structure of the material such that the smaller pores are occupied more effortlessly and consecutively larger pores are occupied as pressure is increased. When the saturation point is approached, i.e. P/P_0 is approximately 1.0, the internal pore structure of the material contains condensed (liquid) nitrogen.

4.5 Fourier Transform Infrared Spectroscopy

Fourier transform infrared spectroscopy (FTIR) is one of the most powerful tools for the identification of compounds by the corresponding spectrum of unidentified compounds with a reference spectrum (finger printing) and investigation of functional groups in an unknown compound. The infrared section of the electromagnetic spectrum is considered to cover the range from 50 to approximately 12,500 cm^{-1}.

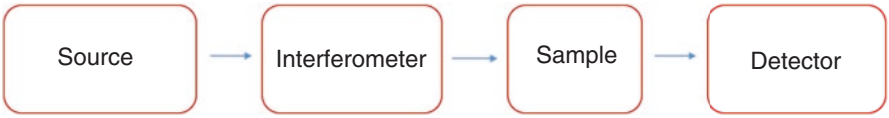

Fig. 16.11 Schematic representations of a Fourier transfer infrared spectroscopy

4.5.1 Basic Principle

In this instrument, when infrared light is accepted through a sample of an organic compound, particular frequencies are absorbed, whereas other frequencies are transmitted without being absorbed. During this procedure, the transitions involved in the infrared absorption are related to the vibrational variations in the molecule. Different bonds/functional groups occur at different vibrational frequencies and hence the occurrence of these vibrational bands in a molecule can be distinguished by identifying this characteristic frequency as an absorption band in the infrared spectrum. The plot spectrum in infrared spectroscopy between transmittance and frequency is called the infrared spectrum.

4.5.2 Instrumentation

Owing to the remarkable speed and sensitivity of FTIR spectrometers have substituted dispersive instruments for maximum applications. They have significantly prolonged the aptitudes of infrared spectroscopy and have been applied to many areas that are very problematic or impossible to investigate using dispersive instruments. Instead of observing each component frequency sequentially, as in a dispersive IR spectrometer, all frequencies are studied at the same time in FTIR spectroscopy. In this instrument, there are three main basic spectrometer components: radiation source, interferometer and detector. The well-designed block shape of the FTIR spectrometer is shown in Fig. 16.11. The source of IR radiation is a broadband source that is first focused into an interferometer, where it is separated and then recombined after the split beams have travelled dissimilar optical paths to generate constructive and destructive interference. The next step is the resulting beam being permitted through the sample compartment and reaching the detector. The preparation of the sample is very easy. Using this technique, almost any samples such as solids, liquids or gases, can be investigated. The sample to be investigated (minimum of 10 μg) should be crushed into a KBr matrix or dissolved in an appropriate solvent (CCl_4 and CS_2 are desired). The exclusion of water from the sample is possible. In the case of solid samples, these are directly mixed with solid KBr pallets (transparent in the mid-infrared region), then crushed and pressed. FTIR measurements were implemented using a Perkin Elmer FTIR spectrophotometer with a standard KBr pellet technique.

4.6 UV-Visible Spectroscopy

Ultraviolet-visible (UV-Vis) spectroscopy refers to absorption spectroscopy in the ultra-violet and visible spectral region. The electronic transition is found in the molecules as the electromagnetic spectrum was present in this region. When sample molecules are uncovered to light with energy (E = hν where E is energy in joules, h is Planck's constant 6.62×10^{-34}Js and ν is frequency in Hertz), which matches a probable electronic transition contained by the molecule, a certain amount of the light energy will be absorbed as the electron is promoted to an upper energy orbital. When the absorption occurs by a molecule at a particular wavelength, it is recorded by an optical spectrometer, simultaneously with the amount of absorption at every wavelength. The resultant spectrum exists as a graph of absorbance (A) versus wavelength (λ). Investigation of the optical properties of NPs can be studied with the help of UV-Vis spectra.

4.6.1 Basic Principle

The absorption of light by molecules in the solution is centred on the Beer–Lambert law,

$$A = I / I_0 = \varepsilon bc$$

where, I_0 is the intensity of the reference beam and I is the intensity of the sample beam, ε is the molar absorptivity with units of L mol^{-1} cm^{-1}, b = route length of the sample in centimetres and c = concentration given the solution expressed in mol L^{-1}.

4.6.2 Instrumentation

In this instrument, the main components are a light source, double beams (reference and sample beams), a monochromator, a detector and a recording device. The light source is usually a tungsten filament lamp used for visibility and a deuterium discharge bulb is used for UV measurements. The light coming out from the light source is divided into dual beams, the reference and the sample beams, as shown in the Fig. 16.12. The sample and reference cells are the rectangular quartz/glass containers; they are filled with the solution (to be tested) and pure solvent respectively. This spectrometer records the proportion between the reference and sample beam intensities. The recorder plots the absorbance (A) against the wavelength (λ). The sample is prepared by proper grinding into a mortar paste and then liquefied into the solvent to form a dilute sample solution. This sample solution is filled with sample cells to the mark line. In the present work, UV-Vis absorption examinations were carried out by a Varian Cary 100 E UV-Vis-NIR spectrophotometer and a Shimadzu (Japan) 3100 PC spectrophotometer using ethanol as a dispersing medium.

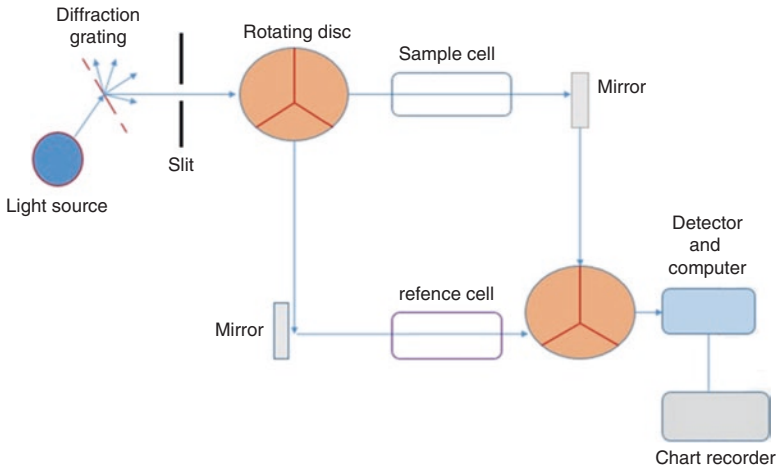

Fig. 16.12 Schematic representation of a ultraviolet-visible spectroscopy

4.7 Photoluminescence Spectroscopy

Photoluminescence spectroscopy is a contactless, non-destructive method for the examination of the electronic structure of materials. This technique is used for the concentration and spectral content of the emitted photoluminescence is an undeviating quantity of immeasurably important material properties, together with band gap determination, contamination levels, imperfection detection and recombination mechanisms.

4.7.1 Basic Principle

Light is concentrated onto a sample, where it is absorbed and imparts additional energy into the material using a method called photo-excitation. Photo-excitation causes electrons contained by a material to transfer into acceptable excited states. These excited electrons come back from their equilibrium states, by a radiative process (the emission of light) or by a non-radiative process, as shown in Fig. 16.13. The quantity of emitted light is associated with the relative contribution of the radiative process.

4.7.2 Instrumentation

The photoluminescence instruments include three elementary items: a cause of light, a sample holder and a detector. A schematic demonstration of a fluorimeter is shown in Fig. 16.14. The light source produces light photons over a broad energy spectrum; in this instrument, the spectra range from 200 to 900 nm. Photons impinge

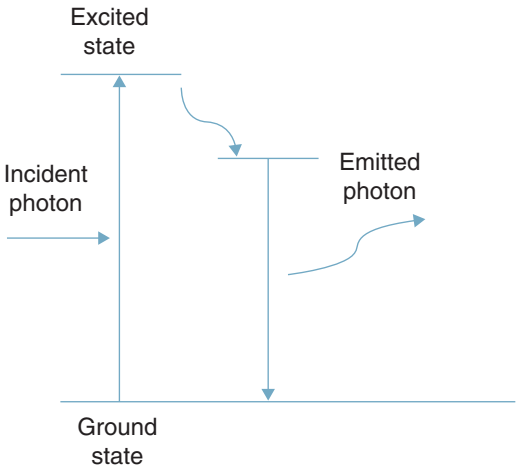

Fig. 16.13 Schematic representation of a principle of photoluminescence (PL) spectra

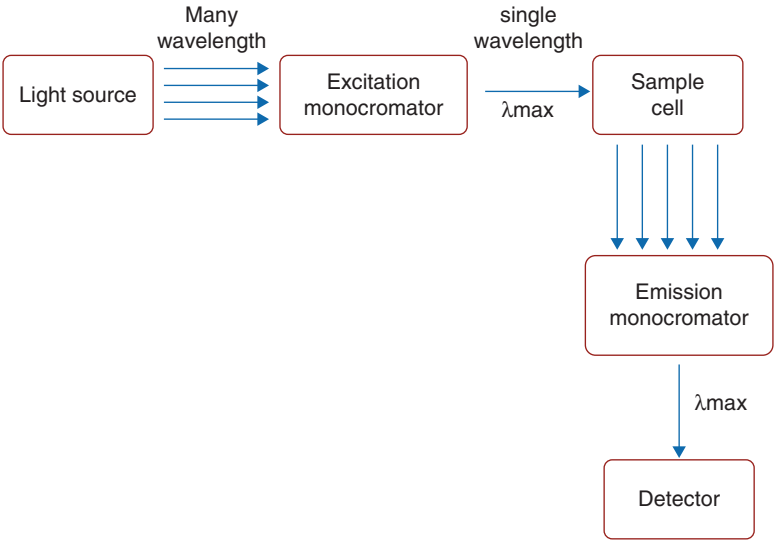

Fig. 16.14 Schematic representations of PL spectra

on the excitation monochromator, which selectively transfers light within a constricted range centred around the excitation wavelength indicated. The transmitted light is permitted through modifiable slits that govern the magnitude and resolution by further restricting the range of transmitted light. In this instrument, the strained light passes through into the sample cells affecting the fluorescent radiation by fluorophores within the sample. Emitted light enters the emission monochromator, which is situated at a 90° angle from the excitation light path to eradicate background signal and decrease the sound owing to stray light. Yet again, emitted light is transmitted within a contracted range centred around the definite emission

wavelength and exiting through adjustable slits, finally entering the photomultiplier tube (PMT). The signal is improved and produces a voltage that is proportional to the measured emitted intensity. The noise arises primarily in the PMT. Therefore, spectral resolutions and signal to noise is directly interconnected to the particular slit widths. The preparation of a sample procedure is the identical to that of UV-Vis spectroscopy. In both cases, it is essential for the sample cell (cuvette) to be free from contaminants. For the present research work, a Fluorolog-3-11 spectrophotometer was employed for photoluminescence measurements.

5 Application of Nanoparticles in Environmental vWaste Management

For environmental waste management, a number of commercial and non-commercial scientific improvements are employed on a daily basis, but nanotechnology has revealed progressive methods of water/wastewater treatment. In the development of nanoscience research, it has to been possible to come up with economically attainable and environmentally stable treatment technologies to dramatically consider water/wastewater contest to improve water quality standards.

Over the past few years, the consumption of NPs as adsorbents, nanosized zero valent ions or nanofiltration membranes has been for the removal/separation of contaminants from water, whereas currently, NPs used as photocatalysts for chemical or photochemical oxidation effect the annihilation of contaminants. The remediation of toxic waste present in air through nanotechnology is carried out in the several ways. One is by the management of nano-photocatalysts, in addition to a simple catalyst with an enhanced surface area for gaseous reactions. Catalysts increase the frequency of chemical reactions that convert harmful gases that have evolved from automobiles and industrial plants into harmless gases. Presently, nanofiber catalysts are applicable and are mostly made of manganese oxide, which discards contaminated organic compounds from industrial smokestacks. The development of other methods is static. An additional way is to approach nanostructure membranes that have smaller pores adequate for separating marsh gas or carbon dioxide from exhausts.

5.1 Role of Nanoparticles in Wastewater Treatment

In terms of wastewater treatment, NPs are applied for the eradication of various forms of waste. Organic contaminants and substantial metal toxic waste pose serious problems to the environment because they are toxic to living beings, including humans, and are not naturally degradable. Several nanomaterials such as TiO_2, ZnO, ceramic membranes, nanowire membranes, polymer membranes, CNTs, submicron

nanopowder, metal (oxides), magnetic NPs, nanostructured boron-doped diamond are used for photocatalysis, nanofiltration, adsorption and electrochemical oxidation to resolve or greatly diminish problems involving water excellence in the natural environment.

5.1.1 Role of Nanoparticles in Removal of Organic Pollutants from Wastewater

Nanoparticles are utilised for the elimination of organic pollutants, which have size-dependent properties correlating with the specific surface area, such as fast dissolution, high reactivity, and strong sorption. Most of the applications discussed below are still in the laboratory research phase. The pilot-tested or field-tested exceptions are noted in the text.

5.1.1.1 Photocatalysis

Photocatalytic oxidation is a forward-looking and recently used oxidation technique for the degradation of toxic pollutants and microbial pathogens. It is a relevant pretreatment for harmful and toxic hazardous materials, which are non-biodegradable pollutants, to enhance their biodegradability in the environment. For the degradation of unruly organic pollutants NPs can also be used as photocatalysts. The most important obstacle to its widespread utilisation is limited because of lighting consequences and photocatalytic activity is slow kinetics. Present research concentrates on enhancing the frequency of photocatalytic reaction and the photoactivity area.

5.1.1.2 TiO_2 Metal Oxide Nanoparticles

TiO_2 NPs are mostly used as water/wastewater treatment semiconductor photocatalysts owing to their low toxicity, their stability, low cost, and also the large amount of raw materials present in nature. On the radiation from UV light, its electrons migrated from the valence band to the conduction band. During the movement of electrons from the valence band to the conduction band, holes (h^+) are created in the valance band and electrons (e^-) in the conduction band. This means it produces an electron/hole (e^-/h^+) pair, which either transfers to the surface and reacts with environmental oxygen to form reactive oxygen species (ROS) or go through undesired recombination. The photocatalytic activity of TiO_2 NPs can be enhanced by controlling the diameter and shape of the particle, reducing e^-/h^+ pair recombination by noble/transition metal doping (Han et al. 2009; Murakami et al. 2009; Liu et al. 2011), maximising the reactive characteristic and surface behaviour to improve pollutant adsorption. The shape, size and morphology of TiO_2 plays a momentous role in its solid-phase conversion, sorption and e^-/h^+ recombination. Amid crystalline TiO_2, rutile is the most reliable and larger than 35 nm, while an anatase, more

valuable in producing ROS, is the most stable for particles smaller than 11 nm (Fujishima et al. 2008; Banfield et al. 2000). A major cause for the slow rate of photodegradation of pollutants by TiO_2 photocatalysis is the rapid recombination of e^- and h^+. Decreasing the size of TiO_2 NPs diminished its recombination of the e^-/h^+ pair, and appreciated its interfacial charge carrier transfer (Zhang et al. 2000). However, when the size of the NPs is decreasing at certain nanometres, surface recombination dominated, and increased its photocatalytic activity. Therefore, the photocatalytic degradation efficiency of the TiO_2 NPs has been maximised because of the interplay of the above-mentioned mechanisms, which lies in the nanometre rang. In the degradation process of organic compounds, the nanotubes of TiO_2 became more capable than TiO_2 NPs (Macak et al. 2007). The advanced photocatalytic activity was accredited to the smaller carrier diffusion paths in the tube walls and the rate of mass transfer of reactants toward the surface of the nanotubes was very fast.

5.1.1.3 Nanosorption

Adsorption is usually used as a polishing step in water and wastewater management to eliminate organic and inorganic pollutants. The capability of traditional adsorbents is consistently defined by the surface area or active sites, the absence of distinction and the degree of adsorption. NPs, which are used as nano-adsorbents, attempt powerful enhancement with their large surface area and sorption sites, small intra-particle diffusion distance, pore size and surface chemistry.

5.1.1.4 Carbon-Based Nano-Adsorbents

Recently, CNTs have demonstrated greater adaptability for the exclusion of organic pollutants than activated carbon on adsorption of several organic pollutants (Pan and Xing 2008). Owing to the extraordinarily precise surface area, the adsorption capability of CNTs with pollutant is high. The adsorption phenomena occur on the particular CNTs at finite surface area is the external surface phenomena (Yang and Xing 2010). In the solution phase, owing to the hydrophilic nature of graphitic surface CNTs loosely aggregating and decreasing the effective surface area. In another way, the aggregation of CNTs consists of interstitial spaces that have a tremendous amount of adsorption energy for adsorption of organic molecules (Pan and Xing 2008). In comparison with CNT, activated carbon also acquired an analogous measured specific surface area and accommodated a considerable number of micropores unattainable to heavy organic pollutants such as various antibiotics and pharmaceuticals. Thus, CNTs have considerably more capability for the adsorption of heavy organic pollutants because of their larger pores in bundles and more available sorption sites.

A considerable deficiency of activated carbon is its low adsorption capacity for the small molecular weight of polar organic compounds. Owing to the different types of CNT interaction such as hydrophobic effect, π–π interactions, hydrogen bonding, covalent bonding and electrostatic interactions, CNTs powerfully adsorb polar organic compounds to form varied contaminated CNTs. The easier availability of π electrons on the CNT surface enable it to interact with π–π interactions with organic molecules through C=C bonds or aromatic rings, such as PAHs and polar aromatic compounds. Many organic compounds contain -COOH, -OH and $-NH_2$ as functional groups that could interact through hydrogen bonds with the graphitic CNT surface, which donates electrons. Within an appropriate pH range, the electrostatic attraction encourages the adsorption of positively charged organic chemicals such as some antibiotics (Qu et al. 2013).

5.1.1.5 Zero-Valent Iron

Metal oxide NPs, including semiconductor materials, bimetallic NPs and zero-valence metals, have been applicable for the degradation of environmental pollutants, for instance PCBs, pesticides, and azo dyes, as a result of their greater surface area and shape-reliant properties (Zhao et al. 2011). The NPs, which behave as magnetic nanosorbents, have also been demonstrated to be adequate for the degradation of organic pollutants (Campos et al. 2011). Among the magnetic nanosorbents, iron oxide nanomaterials have demonstrated a superior degradation efficiency for organic contaminants compared with bulk materials (Li et al. 2003a; Wu et al. 2005; Lai and Chen 2001). For the discharge of coloured humic acid from the wastewater, magnetic Fe_2O_3 NPs have also been applied (Qiao et al. 2003). Usefully, conversion of chlorinated organic contaminants and PCBs has been carried out by applying nano zero valent iron (n-ZVI) (Wang and Zhang 1997; Zhang et al. 1998; Cheng et al. 2007) in addition to inorganic pollutants ions such as nitrate and perchlorate (Choe et al. 2000). NPs of n-ZVI have been revealed as powerful substances for the removal of hazardous chlorinated organic contaminants, for example, 2,2′-dichlorobiphenyl in a minor remediation investigation (Parra et al. 2004). The more reliable n-ZVI NPs could also be a practical technique for in situ remediation of groundwater or industrial toxic wastes. The simple n-ZVI and nanocomposite n-ZVI have appeared as practical redox media for compressing a range of organic contaminants such as PCBs, organic dyes, pesticides, chlorinated hydrocarbon and inorganic toxic anions, e.g. nitrates in water/wastewater because of the large surface areas and high reactivity (Schrick et al. 2002). Many bimetallic NPs such as Ni^0/Fe^0 and Pd^0/Fe^0 were found to be more impressive than general microscale Fe for reducing the halogenation of chlorinated organic pollutants and brominated hydrocarbon, hydro-dechlorination of chlorinated saturated hydrocarbon, chlorinated aromatics and PCBs, as explained by many researchers (Wei et al. 2006; Lim et al. 2007).

5.1.2 Role of Nanoparticles in Elimination of Heavy Metals from Wastewater

Various types of NPs such as CNTs, zeolites, dendrimers and nanosorbents have been identified for the subtraction of heavy metals from water/wastewater because of their exceptional adsorption properties (Amin et al. 2014). The ability of CNTs to adsorb heavy metals has been analysed by many researchers such as $Pb^{2+,}$ $Cu^{2+,}$ Cd^{2+} (Li et al. 2003b), Cr^{3+} (Di et al. 2006) and Zn^{2+} (Lu et al. 2006), and metalloids such as arsenic (As) compounds. The elimination of heavy metal ions by the composites of CNTs with Fe and cerium dioxide (CeO_2) have also been reported in a few studies (Salipira et al. 2007). NPs of cerium dioxide supported on CNTs are effectively applicable to adsorbing arsenic. The fast rate of adsorption on CNTs is primarily because of the high availability of adsorption sites on the surface and the short intra-particle diffusion distance. Metal oxide-based NPs were demonstrated to be superior in discarding toxic heavy metals in comparison with activated carbon, for example, adsorption of arsenic on the surface of nanosized TiO_2 and NPs of magnetite (Deliyanni et al. 2003; Mayo et al. 2007). The application of TiO_2 NPs as photocatalysts has been considered in detail to reduce the harmful metal ions in water (Kabra et al. 2004). In one study, the presentation of NPs of TiO_2 in reducing various forms of arsenic is explained in more detail and they have been shown to be additional impressive photocatalysts compared with generally accessible TiO_2 NPs with a maximum eradication capability of arsenic at about neutral pH value (Pena et al. 2005). The reduction of Cr(VI) to Cr(III) in the presence of sunlight by using a nanocomposite of TiO_2 NPs attached to a graphene sheet and also Cr treatment was implemented by applying palladium NPs in another study (Amin et al. 2014). The efficiency of elimination of poisonous heavy metals such as As (arsenic) is also considered by the use of the low-cost adsorbent iron oxide nanomaterials (Fe_2O_3 and Fe_3O_4) by several researchers (Lai and Chen 2001; Onyango et al. 2003; Oliveira et al. 2004). Further elimination of arsenic was also examined by application of an extraordinary specific surface area of Fe_3O_4 nanocrystals (Yavuz et al. 2006). Implantation of polymer onto Fe_2O_3 was a powerful nanocomposite for the elimination of divalent toxic heavy metal ions for copper, nickel and cobalt in a pH range of up to 3–7 pH (Takafuji et al. 2004). For the elimination of radioactive metal toxins, uranium dioxide (UO_2^{2+}) from water by application of bisphosphonate-modified magnetite NPs was also studied (Inbaraj and Chen 2012). There are more studies that have explained that NPs of n-ZVI or Fe^0 are useful for the conversion of toxic heavy metal ions such as Cd(II), As(V), Pb(II), Cu(II), Ni(II) and Cr(VI) (Zou et al. 2016).

Innovative self-assembled 3D flower-like structures of iron oxide and CeO_2 NPs were also applicable for the good adsorbtion of both As and Cr (Zhong et al. 2006, 2007). The adaptability of NaP1 zeolites was assessed for the elimination of heavy metals (Cr(III), Ni(II), Zn(II), Cu(II) and Cd(II)) from wastewater (Moreno et al. 2001; Alvarez-Ayuso et al. 2003). Polymer-incorporated NPs are also most applicable for the remediation of noxious heavy metal ions (Diallo et al. 2004). The application of mesoporous to support assembled monolayers for the elimination of

toxic metal ions was also mentioned by many researchers (Mattigod et al. 1999; Yantasee et al. 2003). Moreover, the application of biopolymers has been reported for heavy metal removal from aqueous waste (Kostal et al. 2001). Chitosan nanomaterials was further reported for the sorption of Pb(II) (Qi and Xu 2004).

5.2 *Role of Nanoparticles in the Bioremediation of Petroleum Hydrocarbon*

Owing to the hydrophobic nature of the petroleum hydrocarbons that reduces their solubility in water and enhances the sorption properties of soil micelles that inhibit bioremediation of these compounds. Numerous studies have described the fabrication of biosurfactants by the microorganisms that can inhibit the hydrophobicity of these organic pollutants by reducing the surface tension and appreciating the bioavailability of hydrophobic pollutants to microorganisms, which is very significant in the bioremediation process (Cameotra and Makkar 2010). In the adjoining of small nanomaterials, the bioremediation of hydrocarbon can be appreciated, as they reimburse the oxidation of these compounds, decrease their toxic effect and make suitable for the microbial growth. NPs of peroxides (such as calcium peroxide) increase the suspension and kinetics of hydrocarbons. Applications of calcium peroxide (CaO^2) NPs as an attractive oxidant are treated as honest oxygen discharge material (Northup and Cassidy 2008). A mixture of benzene and gasoline (as high as 800 mg L^{-1}) can be completely oxidised within 24 h (Pereira et al. 2005). Application of iron oxide (FeO) and hydrogen peroxide (H_2O_2) in the proportion of 1:33.7 has been applicable to reduce up to 91% of the total petroleum hydrocarbon within 4 h (Kumari and Singh 2016).

The experiential investigation by Jameia et al. (2013) into the degradation of the hydrocarbon chain in the soil registered an enhanced n-ZVI, whereas manganese and cobalt NPs (MnNP and CoNP) promoted the contraction of PAHs (Nador et al. 2010). The regiochemistry and degree of decrease of derivatives of 1-substituted naphthalene were mainly dependent on the nature of metal NPs used. The NPs of Co encourage the contraction of PAHs, most important to the corresponding tetralin products, whereas the Mn NPs permitted the construction of unconjugated 5,8-dihydro derivatives. Co-NP was found to be more conscious than Mn NPs in the conversion of 9,10-dihydrophenanthrene into phenanthrene within 3 h. The conversion of naphthalene into 1,2,3,4-tetrahydronaphthalene by the reaction of Co NPs at room temperature is a qualitative example.

Nano-titanium oxide is applied as a photocatalyst in the existence of UV light for degradation of organic noxious waste from petroleum refinery wastewater (Saien and Shahrezaei 2012). A very low concentration of this catalyst (100 mg L^{-1}) at pH 3.0 and a temperature of 45 °C could remove about 78% of the organic contaminants (after 60–90 min) in the occurrence of UV irradiation. The degradation of petroleum hydrocarbon by the NPs of the TiO_2 was observed by Fard et al. (2013),

whereas colloidal NPs of TiO_2 for photocatalysis are applicable for the removal of the seawater-soluble crude oil fraction observed by Ziollia and Jardim (2001). The dissolution of organic carbon in the occurrence of TiO_2 removed 90% crude oil compounds in sea water, which contained about 45 mg of carbon L^{-1} of seawater-soluble after 7 days of non-natural light exposure.

6 Conclusion

This chapter concludes that NPs are the preeminent fundamental unit of nanotechnology. They are a group of tens of thousands of atoms measuring about 1–100 nm of a massively ordered crystalline nature. Such NPs originated atom by atom; thus, the size and regularity of the shape, of a particle, are composed of the preliminary conditions. The prerequisite of nanotechnology is to synthesise the desired shape and size of the nanomaterials for their convenient applications. Surfactants play a significant role during the synthesis of NPs. Owing to the huge surface area to volume ratio, nanostructures display distinctive properties.

In nanotechnology, the cost-effective production of NPs has the potential to advance the environment, both through straight utilisation of those materials to distinguish, avoid and eradicate contamination, and indirectly by using nanotechnology to design cleaner industrial routes and generate environmentally accountable products. For instance, ZnO, iron oxide (Fe_2O_3), cobalt oxide (Co_2O_3) and certain other different NPs can remove contaminants from topsoil and ground water, and nano-sized sensors hold assurance for better-quality detection and tracing of contaminants. These nanomaterials provide clean water from contaminated water sources on both an outsized scale and via a transportable application, in addition to detecting and cleaning up eco-friendly contaminants (waste and toxic material), i.e. remediation.

Acknowledgment The authors wish to thank the Babasaheb Bhimrao Ambedkar University (a central University) of U.P India for providing the opportunity to carry out this work.

References

Alvarez-Ayuso E, Garcıa-Sánchez A, Querol X (2003) Purification of metal electroplating waste waters using zeolites. Water Res 37:4855–4862

Amin MT, Alazba AA, Manzoor U (2014) A review of removal of pollutants from water/wastewater using different types of nanomaterials. Adv Mater Sci Eng 190:208–222

Ansari SA, Husain Q (2012) Potential applications of enzymes immobilized on/in nano materials: a review. Biotechnol Adv 30:512–523

Baladi A, Mamoory RS (2010) Investigation of different liquid media and ablation times on pulsed laser ablation synthesis of aluminum nanoparticles. Appl Surf Sci 256:7559–7564

Banfield JF, Welch SA, Zhang H, Ebert TT, Penn RL (2000) Aggregation-based crystal growth and microstructure development in natural iron oxyhydroxide biomineralization products. Science 289:751–754

Bhattacharya S, Saha I, Mukhopadhyay A, Chattopadhyay D, Chand U, Chatterjee D (2013) Role of nanotechnology in water treatment and purification: potential applications and implications. Int J Chem Sci Technol 3:59–64

Boldyrev VV, Tkáčová K (2000) Mechanochemistry of solids: past, present, and prospects. J Mater Synth Process 8:121–132

Cameotra SS, Makkar RS (2010) Biosurfactant-enhanced bioremediation of hydrophobic pollutants. Pure Appl Chem 82:97–116

Campos AFC, Aquino R, Cotta T, Tourinho FA, Depeyrot J (2011) Using speciation diagrams to improve synthesis of magnetic nanosorbents for environmental applications. Bull Mater Sci 34:1357–1361

Chen D, Jiao X, Cheng G (1999) Hydrothermal synthesis of zinc oxide powders with different morphologies. Solid State Commun 113:363–366

Cheng R, Wang J, Zhang W (2007) Comparison of reductive dechlorination of p-chlorophenol using Fe0 and nanosized Fe0. J Hazard Mater 144:334–339

Choe S, Chang YY, Hwang KY, Khim J (2000) Kinetics of reductive denitrification by nanoscale zero-valent iron. Chemosphere 41:1307–1311

Daou TJ, Pourroy G, Colin SB et al (2006) Hydrothermal synthesis of monodisperse magnetite nanoparticles. Chem Mater 18:4399–4404

Deliyanni EA, Bakoyannakis DN, Zouboulis AI, Matis KA (2003) Sorption of As (V) ions by akaganéite-type nanocrystals. Chemosphere 50:155–163

Di ZC, Ding J, Peng XJ, Li YH, Luan ZK, Liang J (2006) Chromium adsorption by aligned carbon nanotubes supported ceria nanoparticles. Chemosphere 62:861–865

Diallo MS, Christie S, Swaminathan P et al (2004) Dendritic chelating agents. 1. Cu (II) binding to ethylene diamine core poly (amidoamine) dendrimers in aqueous solutions. Langmuir 20:2640–2651

Djurisic AB, Chen XY, Leung YH (2012) Recent progress in hydrothermal synthesis of zinc oxide nanomaterials. Recent Patents Nanotech 6:124–134

Egerton RF (2005) Physical principles of electron microscopy. Springer, New York

Fard MA, Aminzadeh B, Vahidi H (2013) Degradation of petroleum aromatic hydrocarbons using TiO_2 nanopowder film. Environ Technol 34:1183–1190

Fujishima A, Zhang X, Tryk DA (2008) TiO_2 photocatalysis and related surface phenomena. Surf Sci Rep 63:515–582

Ghorbani HR (2014) A review of methods for synthesis of al nanoparticles. Orient J Chem 30:1941–1949

Gupta K, Bhattacharya S, Chattopadhyay D et al (2011) Ceria associated manganese oxide nanoparticles: synthesis, characterization and arsenic (V) sorption behavior. Chem Eng J 172:219–229

Han X, Kuang Q, Jin M, Xie Z, Zheng L (2009) Synthesis of titania nanosheets with a high percentage of exposed (001) facets and related photocatalytic properties. J Am Chem Soc 131:3152–3153

Hur TB, Phuoc TX, Chyu MK (2009) Synthesis of Mg-Al and Zn-Al-layered double hydroxide nanocrystals using laser ablation in water. Opt Lasers Eng 47:695–700

Inbaraj BS, Chen BH (2012) In vitro removal of toxic heavy metals by poly (γ-glutamic acid)-coated superparamagnetic nanoparticles. Int J Nanomedicine 7:4419–4432

Innes B, Tsuzuki T, Dawkins H et al (2002) Nanotechnology and the cosmetic chemist. Cosmetics Aerosols Toiletries Australia 15:10–24

Jameia MR et al (2013) Degradation of oil from soilusing nano zero valent iron. Sci Int 25:863–867

Jolivet JP, Chanéac C, Tronc E (2004) Iron oxide chemistry. From molecular clusters to extended solid networks. Chem Commun 5:481–483

Josephine A, Nithya K, Amudha G, Veena CK, Preetha SP, Varalakshmi P (2008) Role of sulphated polysaccharides from Sargassum Wightii in cyclosporine A-induced oxidative liver injury in rats. BMC Pharmacol 8:4

Kabra K, Chaudhary R, Sawhney RL (2004) Treatment of hazardous organic and inorganic compounds through aqueous-phase photocatalysis: a review. Ind Eng Chem Res 43:7683–7696
Kermanpur A, Dadfar MR, Rizi BN, Eshraghi M (2010) Synthesis of aluminum nanoparticles by electromagnetic levitational gas condensation method. J Nanosci Nanotechnol 10:6251–6255
Khoshnevisan K, Bordbar AK, Zare D et al (2011) Immobilization of cellulase enzyme on superparamagnetic nanoparticles and determination of its activity and stability. Chem Eng J 171:669–673
Kołodziejczak-Radzimska A, Jesionowski T, Krysztafkiewicz A (2010) Obtaining zinc oxide from aqueous solutions of KOH and Zn $(CH_3COO)_2$. Physicochem Probl Mineral 44:93–102
Kołodziejczak-Radzimska A, Markiewicz AE, Jesionowski T (2012) Structural characterisation of ZnO particles obtained by the emulsion precipitation method. J Nanomater 2012:15
Kostal J, Mulchandani A, Chen W (2001) Tunable biopolymers for heavy metal removal. Macromolecules 34:2257–2261
Kratochvil D, Volesky B (1998) Advances in the biosorption of heavy metals. Trends Biotechnol 16:291–300
Kumari B, Singh DP (2016) A review on multifaceted application of nanoparticles in the field of bioremediation of petroleum hydrocarbons. Ecol Eng 97:98–105
Kumari V, Yadav A, Haq I, Kumar S, Bharagava RN, Singh SK, Raj A (2016) Genotoxicity evaluation of tannery effluent treated with newly isolated hexavalent chromium reducing Bacillus Cereus. J Environ Manag 183:204–211
Lai CH, Chen CY (2001) Removal of metal ions and humic acid from water by iron-coated filter media. Chemosphere 44:1177–1184
LaMer VK (1952) Nucleation in phase transitions. Ind Eng Chem Res 44:1270–1277
LaMer VK, Dinegar RH (1950) Theory, production and mechanism of formation of monodispersed hydrosols. J Am Chem Soc 72:4847–4854
Laurent S, Forge D, Port M et al (2008) Magnetic iron oxide nanoparticles: synthesis, stabilization, vectorization, physicochemical characterizations, and biological applications. Chem Rev 108:2064–2110
Lee W, Kim MG, Choi J et al (2005) Redox-transmetalation process as a generalized synthetic strategy for core-shell magnetic nanoparticles. J Am Chem Soc 127:16090–16097
Li P, Miser DE, Rabiei S, Yadav RT, Hajaligol MR (2003a) The removal of carbon monoxide by iron oxide nanoparticles. Appl Catal B 43:151–162
Li YH, Ding J, Luan Z et al (2003b) Competitive adsorption of Pb^{2+}, Cu^{2+} and Cd^{2+} ions from aqueous solutions by multiwalled carbon nanotubes. Carbon 41:2787–2792
Li X, He G, Xiao G, Liu H, Wang M (2009) Synthesis and morphology control of ZnO nanostructures in microemulsions. J Colloid Interface Sci 333:465–473
Lifshitz IM, Slyozov VV (1961) The kinetics of precipitation from supersaturated solid solutions. J Phys Chem Solids 19:35–50
Lim TT, Feng J, Zhu BW (2007) Kinetic and mechanistic examinations of reductive transformation pathways of brominated methanes with nano-scale Fe and Ni/Fe particles. Water Res 41:875–883
Liu S, Yu J, Jaroniec M (2011) Anatase TiO_2 with dominant high-energy {001} facets: synthesis, properties, and applications. Chem Mater 23:4085–4093
Liu M, Wang Z, Zong S et al (2014) SERS detection and removal of mercury (II)/silver (I) using oligonucleotide-functionalized core/shell magnetic silica sphere@ Au nanoparticles. ACS Appl Mater Interfaces 6:7371–7379
Lowell S, Shields JE, Thomas MA, Thommes M (2004) Surface area analysis from the Langmuir and BET theories. Characterization of porous solids and powders: surface area, pore size and density. Particle Technology Series, vol 16. Springer, Dordrecht
Lu C, Chiu H, Liu C (2006) Removal of zinc (II) from aqueous solution by purified carbon nanotubes: kinetics and equilibrium studies. Ind Eng Chem Res 45:2850–2855
Macak JM, Stein FS, Schmuki P (2007) Efficient oxygen reduction on layers of ordered TiO_2 nanotubes loaded with Au nanoparticles. Electrochem Commun 9:1783–1787

Mahato TH, Prasad GK, Singh B, Acharya J, Srivastava AR, Vijayaraghavan R (2009) Nanocrystalline zinc oxide for the decontamination of sarin. J Hazard Mater 165:928–932
Mansoori GA (2002) Advances in atomic & molecular nanotechnology. United Nations Tech Monitor; UN-APCTT Tech Monitor, 2002; Special Issue: 53 59
Masciangioli T, Zhang WX (2003) Peer reviewed: environmental technologies at the nanoscale. Environ Sci Technol 37:102A–108A
Mattigod SV, Feng X, Fryxell GE, Liu J, Gong M (1999) Separation of complexed mercury from aqueous wastes using self-assembled mercaptan on mesoporous silica. Sep Sci Technol 34:2329–2345
Mayo JT, Yavuz C, Yean S et al (2007) The effect of nanocrystalline magnetite size on arsenic removal. Sci Technol Adv Mater 8:71–75
Mehndiratta P, Jain A, Srivastava S, Gupta N (2013) Environmental pollution and nanotechnology. Environ Pollut 2:49
Mizutani N, Iwasaki T, Watano S, Yanagida T, Tanaka H, Kawai T (2008) Effect of ferrous/ferric ions molar ratio on reaction mechanism for hydrothermal synthesis of magnetite nanoparticles. Bull Mater Sci 31:713–717
Moreno N, Querol X, Ayora C, Pereira CF, Janssen-Jurkovicová M (2001) Utilization of zeolites synthesized from coal fly ash for the purification of acid mine waters. Environ Sci Technol 35:3526–3534
Murakami N, Kurihara Y, Tsubota T, Ohno T (2009) Shape-controlled anatase titanium (IV) oxide particles prepared by hydrothermal treatment of peroxo titanic acid in the presence of polyvinyl alcohol. J Phys Chem C 113:3062–3069
Nador F, Moglie Y, Vitale C, Yus M, Alonso F, Radivoy G (2010) Reduction of polycyclic aromatic hydrocarbons promoted by cobalt or manganese nanoparticles. Tetrahedron 66:4318–4325
Nirmala MJ, Shiny PJ, Ernest V et al (2013) A review on safer means of nanoparticle synthesis by exploring the prolific marine ecosystem as a new thrust area in nanopharmaceutics. Int J Pharm Sci 5:23–29
Northup A, Cassidy D (2008) Calcium peroxide (CaO_2) for use in modified Fenton chemistry. J Hazard Mater 152:1164–1170
Oliveira LCA, Petkowicz DI, Smaniotto A, Pergher SBC (2004) Magnetic zeolites: a new adsorbent for removal of metallic contaminants from water. Water Res 38:3699–3704
Onyango MS, Kojima Y, Matsuda H, Ochieng A (2003) Adsorption kinetics of arsenic removal from groundwater by iron-modified zeolite. J Chem Eng Jpn 36:1516–1522
Ostwald W (1900) Über die vermeintliche Isomerie des roten und gelben Quecksilberoxyds und die Oberflächenspannung fester Körper. Z Phys Chem 34:495–503
Pan B, Xing B (2008) Adsorption mechanisms of organic chemicals on carbon nanotubes. Environ Sci Technol 42:9005–9013
Parra S, Stanca SE, Guasaquillo I, Thampi KR (2004) Photocatalytic degradation of atrazine using suspended and supported TiO_2. Appl Catal B 51:107–116
Pena ME, Korfiatis GP, Patel M, Lippincott L, Meng X (2005) Adsorption of As (V) and As (III) by nanocrystalline titanium dioxide. Water Res 39:2327–2337
Pereira KRO et al (2005) Brazilian organoclays as nanostructured sorbents of petroleum-derived hydrocarbons. Mat Res 8:77–80
Qi L, Xu Z (2004) Lead sorption from aqueous solutions on chitosan nanoparticles. Colloids Surf A Physicochem Eng Asp 251:183–190
Qiao S, Sun DD, Tay JH, Easton C (2003) Photocatalytic oxidation technology for humic acid removal using a nano-structured TiO_2/Fe_2O_3 catalyst. Water Sci Tech 47:211–217
Qu X, Alvarez PJJ, Li Q (2013) Applications of nanotechnology in water and wastewater treatment. Water Res 47:3931–3946
Reiss H (1951) The growth of uniform colloidal dispersions. J Chem Phys 19:482–487
Ristić M, Musić S, Ivanda M, Popović S (2005) Sol-gel synthesis and characterization of nanocrystalline ZnO powders. J Alloys Compd 397:L1–L4
Rizwan M, Singh M, Mitra CK, Morve RK (2014) Ecofriendly application of nanomaterials: Nanobioremediation. J Nanopart Res 2014

Saien J, Shahrezaei F (2012) Organic pollutants removal from petroleum refinery wastewater with nanotitania photocatalyst and UV light emission. Int J Photoenergy 2012:1

Salipira KL, Mamba BB, Krause RW, Malefetse TJ, Durbach SH (2007) Carbon nanotubes and cyclodextrin polymers for removing organic pollutants from water. Environ Chem Lett 5:13–17

Schrick B, Blough JL, Jones AD, Mallouk TE (2002) Hydrodechlorination of trichloroethylene to hydrocarbons using bimetallic nickel-iron nanoparticles. Chem Mater 14:5140–5147

Schrick B, Hydutsky BW, Blough JL, Mallouk TE (2004) Delivery vehicles for zerovalent metal nanoparticles in soil and groundwater. Chem Mater 16:2187–2193

Schwarzer HC, Peukert W (2004) Tailoring particle size through nanoparticle precipitation. Chem Eng Commun 191:580–606

Shao D, Sheng G, Chen C, Wang X, Nagatsu M (2010) Removal of polychlorinated biphenyls from aqueous solutions using β-cyclodextrin grafted multiwalled carbon nanotubes. Chemosphere 79:679–685

Sugimoto T (2007) Underlying mechanisms in size control of uniform nanoparticles. J Colloid Interface Sci 309:106–118

Takafuji M, Ide S, Ihara H, Xu Z (2004) Preparation of poly (1-vinylimidazole)-grafted magnetic nanoparticles and their application for removal of metal ions. Chem Mater 16:1977–1983

Thanh NTK, Maclean N, Mahiddine S (2014) Mechanisms of nucleation and growth of nanoparticles in solution. Chem Rev 114:7610–7630

Van Dillewijn P, Caballero A, Paz JA, González-Pérez MM, Oliva JM, Ramos JL (2007) Bioremediation of 2, 4, 6-trinitrotoluene under field conditions. Environ Sci Technol 41:1378–1383

Vorobyova SA, Lesnikovich AI, Mushinskii VV (2004) Interphase synthesis and characterization of zinc oxide. Mater Lett 58:863–866

Wagner C (1961) Theorie der alterung von niederschlägen durch umlösen (Ostwald-reifung). Zeitschrift für Elektrochemie, Berichte der Bunsengesellschaft für physikalische Chemie 65:581–591

Wang CB, Zhang WX (1997) Synthesizing nanoscale iron particles for rapid and complete dechlorination of TCE and PCBs. Environ Sci Technol 31:2154–2156

Wang J, Peng Z, Huang Y, Chen Q (2004) Growth of magnetite nanorods along its easy-magnetization axis of [110]. J Cryst Growth 263:616–619

Wang Y, Zhang C, Bi S, Luo G (2010) Preparation of ZnO nanoparticles using the direct precipitation method in a membrane dispersion micro-structured reactor. Powder Technol 202:130–136

Watzky MA, Finke RG (1997) Transition metal nanocluster formation kinetic and mechanistic studies. A new mechanism when hydrogen is the reductant: slow, continuous nucleation and fast autocatalytic surface growth. J Am Chem Soc 119:10382–10400

Wei J, Xu X, Liu Y, Wang D (2006) Catalytic hydrodechlorination of 2, 4-dichlorophenol over nanoscale Pd/Fe: reaction pathway and some experimental parameters. Water Res 40:348–354

Wu R, Qu J, Chen Y (2005) Magnetic powder MnO-Fe_2O_3 composite-a novel material for the removal of azo-dye from water. Water Res 39:630–638

Yadav TP, Yadav RM, Singh DP (2012) Mechanical milling: a top down approach for the synthesis of nanomaterials and nanocomposites. J Nanosci Nanotechnol 2:22–48

Yadav A, Chowdhary P, Kaithwas G, Bharagava RN (2017) Toxic metals in environment, threats on ecosystem and bioremediation approaches. In: Das S, Dash HR (eds) Handbook of metal-microbe interactions and bioremediation. CRC Press, Taylor & Francis Group, Boca Raton, p 813

Yang K, Xing B (2010) Adsorption of organic compounds by carbon nanomaterials in aqueous phase: polanyi theory and its application. Chem Rev 110:5989–6008

Yantasee W, Lin Y, Fryxell GE, Busche BJ, Birnbaum JC (2003) Removal of heavy metals from aqueous solution using novel nanoengineered sorbents: self-assembled carbamoylphosphonic acids on mesoporous silica. Sep Sci Technol 38:3809–3825

Yavuz CT, Mayo JT, William WY et al (2006) Low-field magnetic separation of monodisperse Fe_3O_4 nanocrystals. Science 314:964–967

Zhang W, Wang CB, Lien HL (1998) Treatment of chlorinated organic contaminants with nanoscale bimetallic particles. Catal Today 40:387–395

Zhang Q, Gao L, Guo J (2000) Effects of calcination on the photocatalytic properties of nanosized TiO_2 powders prepared by $TiCl_4$ hydrolysis. Appl Catal B 26:207–215

Zhang WX (2003) Nanoscale iron particles for environmental remediation: an overview. J Nanopart Res 5:323–332

Zhang J, Wang J, Zhou S et al (2010) Ionic liquid-controlled synthesis of ZnO microspheres. J Mater Chem 20:9798–9804

Zhao X, Lv L, Pan B, Zhang W, Zhang S, Zhang Q (2011) Polymer-supported nanocomposites for environmental application: a review. Chem Eng J 170:381–394

Ziolli RL, Jardim WF (2001) Photocatalytic decomposition of seawater-soluble crude oil fractions using high surface area colloid nanoparticles of TiO_2. J Photochem Photobiol 5887:1–8

Zhong LS, Hu JS, Liang HP, Cao AM, Song WG, Wan LJ (2006) Self-assembled 3D flowerlike iron oxide nanostructures and their application in water treatment. Adv Mater 18:2426–2431

Zhong LS, Hu JS, Cao AM, Liu Q, Song WG, Wan LJ (2007) 3D flowerlike ceria micro/nanocomposite structure and its application for water treatment and CO removal. Chem Mater 19:1648–1655

Zou Y, Wang X, Khan A et al (2016) Environmental remediation and application of nanoscale zero-valent iron and its composites for the removal of heavy metal ions: a review. Environ Sci Technol 50:7290–7304